Performance Evaluation of Beamformed Spatial Multiplexing Transmission in Millimeter-Wave Communication Channels

Seung Joon Lee
Department of Electrical & Electronic Engineering
Kangwon National University
Chuncheon 200-701, Korea
Email: s.j.lee@ieee.org

Wooyong Lee, Seung-Eun Hong, and Jinkyeong Kim
Future Communications Research Laboratory
Electronics & Telecommunications Research Institute
Daejeon 305-700, Korea
Email: wylee@etri.re.kr

***Abstract*—This article deals with the study on the performance of the hybrid transmission scheme combining both beamforming and spatial multiplexing. Specifically, the capacity of the hybrid scheme is evaluated and compared to that of the just beamforming scheme in line-of-sight and multi-path channels. Two kinds of the hybrid schemes are considered: the shared antenna architecture where each antenna processes all data streams and the split antenna architecture where each antenna processes only one data stream. The effects of the channel parameters such as the antenna spacing, the existence of reflecting paths, etc. on the capacity and the optimal beams and powers are examined. The frequency-selectivity property of the capacity and the optimal beams and powers is also investigated. In this study, a scenario is considered where the same analog RF beamformer is applied to all subcarriers but the digital baseband power allocation is executed individually at each subcarrier.**

***Index Terms*—60 GHz, beamforming, millimeter-wave, MIMO, spatial multiplexing.**

I. Introduction

Millimeter-wave communications are considered to be very promising technologies for the provision of wireless giga-bits per second service applications, such as uncompressed high-definition video streaming, wireless external computer peripherals, kiosk file down/up-loading, giga-bit WiFi, and so on [1]–[3]. Several standardization activities have been performed for millimeter-wave communication systems, among which IEEE 802.15.3c [3], ECMA [4], WiGig [5], WirelessHD [6], and IEEE 802.11ad [7] are noteworthy.

It is well-known that employing multiple antennas results in a significant increase in the capacity of radio channels with rich scattering [8], [9]. On the other hand, the scattering effect is reduced but the specular reflection is amplified in the millimeter-wave channels [1]. In the channel model [10] adopted by the IEEE 802.11ad study group, the power ratio between scattered and specular components is found to be 10.8%:89.2% [11]. Research results on the MIMO capacity of millimeter-wave line-of-sight or multi-path channels can be found in [11]–[16].

This work was supported by the IT R&D program of ETRI [Development of Millimeter Wave Broadband Wireless Transmission Technologies].

It requires high SNR to achieve a large capacity of MIMO spatial multiplexing. In low SNR environments, a usually considered technique for performance improvement is beamforming, where multiple antennas are used to generate a transmit (TX) or receive (RX) beam, rather than to enable spatial multiplexing [17]. We may consider a hybrid scheme of combining the beamforming and the spatial multiplexing. An academic research result concerning this issue can be found in [18]. However, this approach has not been common in practice but in one exception [6]. In [6], two types of architectures for the hybrid scheme are introduced: The first one is the split antenna architecture as shown in [6, Figure 19], where each antenna is concerned only with one of spatially multiplexed beams. The other is the shared antenna architecture as shown in [6, Figure 20], where each antenna is concerned with all of spatially multiplexed beams. In [18], the former architecture was considered in a line-of-sight channel.

In this paper, we evaluate the capacities of the hybrid schemes in both line-of-sight and multi-path channels, by utilizing the ray-tracing technique [10]. We focus on the dependence of the capacity on the antenna spacing. Also, the effect of reflections on the capacity is examined. In multi-path channels, the frequency-selectivity of the capacity and the optimal beamforming matrices is investigated.

The rest of this paper is organized as follows. In Section II, we describe the model for the hybrid beamforming and spatial multiplexing scheme under consideration. In Section III, we summarize the formulas for the capacity, the optimal beamforming matrices, and the optimal power allocation among multiple spatial streams in the hybrid schemes. In Section IV, the performance of the hybrid beamforming and spatial multiplexing scheme is discussed, based on the presented numerical examples. Finally, conclusion is drawn in Section V.

II. A Model for the Hybrid Beamforming and Spatial Multiplexing System

The hybrid beamforming and spatial multiplexing architecture is assumed to be the same as shown in [6, Figures 19

978-1-4673-1881-5/12/$31.00 ©2012 IEEE

and 20] and it is described as follows. There are M_{TX} transmit (TX) antenna elements and M_{RX} receive (RX) antenna elements. Also, there are P_{TX} TX spatial multiplexing ports and P_{RX} RX spatial multiplexing ports. The number of data streams to be transmitted is denoted by K.

The precoding matrix mapping from K data streams to P_{TX} TX spatial multiplexing ports is denoted by $\mathbf{U}$ of dimension $P_{\mathrm{TX}} \times K$ and the postcoding matrix mapping from P_{RX} RX spatial multiplexing ports to K received data streams is denoted by $\mathbf{V}$ of dimension $K \times P_{\mathrm{RX}}$. Let the channel matrix be $\mathbf{H}$ (dimension $M_{\mathrm{RX}} \times M_{\mathrm{TX}}$) and the TX and RX beamforming matrices be $\mathbf{W}_{\mathrm{TX}}$ (dimension $M_{\mathrm{TX}} \times P_{\mathrm{TX}}$) and $\mathbf{W}_{\mathrm{RX}}$ (dimension $P_{\mathrm{RX}} \times M_{\mathrm{RX}}$), respectively. In the case of the split antenna structure [6, Figure 19], the number of the nonzero entries in $\mathbf{W}_{\mathrm{TX}}$ (or $\mathbf{W}_{\mathrm{RX}}$) is no more than M_{TX} (or M_{RX}), because each antenna element processes only one of multiple spatial streams.

If we let the noise signal vector at the RX antennas be denoted by $\mathbf{n}$ (dimension $M_{\mathrm{RX}} \times 1$) and the transmitted signal for K data streams by $\mathbf{x}$, the signal $\mathbf{y}$ for the received K data streams is represented as

$$\mathbf{y} = \mathbf{V} \cdot \mathbf{W}_{\mathrm{RX}} \left(\mathbf{H} \cdot \mathbf{W}_{\mathrm{TX}} \cdot \mathbf{U} \cdot \mathbf{x} + \mathbf{n} \right). \tag{1}$$

III. Formulas for Capacity, Optimal Beam Matrices, and Power Allocation

The formulas for the capacity, the optimal beamforming matrices and the optimally allocated powers are well documented in [8]. Using the results of [8], the capacity of the system described in Section II is given by (2), shown at the bottom of the page, where $(\ )^{\dagger}$ denotes the complex conjugate transpose of a matrix, $\mathbf{I}_{K \times K}$ denotes the identity matrix of dimension $K \times K$, $|\cdot|$ denotes the determinant of a matrix, and E_s/N_o denotes the total (over all transmit streams) energy per symbol divided by the one-sided noise spectral density.

A. For Shared Antenna Architecture

Based on the singular value decomposition, the channel matrix $\mathbf{H}$ is decomposed as $\mathbf{H} = \mathbf{Q}\mathbf{D}\mathbf{E}^{\dagger}$ where $\mathbf{Q}$ of dimension $M_{\mathrm{RX}} \times M_{\mathrm{RX}}$ and $\mathbf{E}$ of dimension $M_{\mathrm{TX}} \times M_{\mathrm{TX}}$ are the left and right singular matrices, respectively, and $\mathbf{D}$ of dimension $M_{\mathrm{RX}} \times M_{\mathrm{TX}}$ is the rectangular diagonal matrix with singular values on the diagonal. In the case of the shared antenna architecture with $K \leq P_{\mathrm{TX}}$ and $K \leq P_{\mathrm{RX}}$, the theoretically optimal $\mathbf{W}_{\mathrm{TX}}$, $\mathbf{W}_{\mathrm{RX}}$, $\mathbf{U}$, and $\mathbf{V}$ can be obtained as follows [8]: The optimal $\mathbf{W}_{\mathrm{TX}}$ is given by the matrix comprised of the first P_{TX} right singular vectors of $\mathbf{E}$ (i.e., the first P_{TX} columns of $\mathbf{E}$). That is, it is obtained as $\mathbf{W}_{\mathrm{TX}}^{(\mathrm{o})} = \mathbf{E}_{1:P_{\mathrm{TX}}}$ where $(\ )_{1:k}$ denotes the matrix comprised of the first k columns of a given matrix. Similarly, the optimal $\mathbf{W}_{\mathrm{RX}}$ is given by $\mathbf{W}_{\mathrm{RX}}^{(\mathrm{o})} = \mathbf{Q}_{1:P_{\mathrm{RX}}}^{\dagger}$. Then the optimal $\mathbf{U}$ is just given by a rectangular diagonal matrix with the diagonal entries taking care of power allocation based on the water-filling principle [8]. Also, the optimal $\mathbf{V}$ is trivially given by a diagonal matrix with ones on the diagonal.

Since $\mathbf{W}_{\mathrm{TX}}$ and $\mathbf{W}_{\mathrm{RX}}$ are chosen to have $\mathbf{W}_{\mathrm{RX}}\mathbf{H}\mathbf{W}_{\mathrm{TX}}$ diagonal, the optimal $\mathbf{U}$ and $\mathbf{V}$ are diagonal matrices. Unless $\mathbf{W}_{\mathrm{RX}}\mathbf{H}\mathbf{W}_{\mathrm{TX}}$ is diagonal, the optimal $\mathbf{U}$ and $\mathbf{V}$ may not be simply diagonal anymore.

B. For Split Antenna Architecture

In the case of the split antenna architecture, the analytical formulas for the optimal $\mathbf{W}_{\mathrm{RX}}$, $\mathbf{W}_{\mathrm{TX}}$, $\mathbf{U}$ and $\mathbf{V}$ are unavailable. Therefore, we should count on a numerical method for optimization. It can be formulated as follows:

$$\max_{\substack{\mathbf{W}_{\mathrm{TX}}^{(\mathrm{split})}, \mathbf{W}_{\mathrm{RX}}^{(\mathrm{split})}, \mathbf{U}, \mathbf{V} \\ \mathrm{tr}\left\{ \left(\mathbf{W}_{\mathrm{TX}}^{(\mathrm{split})}\mathbf{U}\right) \cdot \left(\mathbf{W}_{\mathrm{TX}}^{(\mathrm{split})}\mathbf{U}\right)^{\dagger} \right\} = 1}} C\left(\mathbf{W}_{\mathrm{TX}}^{(\mathrm{split})}, \mathbf{W}_{\mathrm{RX}}^{(\mathrm{split})}, \mathbf{U}, \mathbf{V} \right) \tag{3}$$

where $C(\mathbf{W}_{\mathrm{TX}}^{(\mathrm{split})}, \mathbf{W}_{\mathrm{RX}}^{(\mathrm{split})}, \mathbf{U}, \mathbf{V})$ is the same as (2) with $\mathbf{W}_{\mathrm{TX}}$ and $\mathbf{W}_{\mathrm{RX}}$ replaced by $\mathbf{W}_{\mathrm{TX}}^{(\mathrm{split})}$ and $\mathbf{W}_{\mathrm{RX}}^{(\mathrm{split})}$ which are such that only one entry within each row of $\mathbf{W}_{\mathrm{TX}}^{(\mathrm{split})}$ and only one entry within each column of $\mathbf{W}_{\mathrm{RX}}^{(\mathrm{split})}$ can be non-zeros.

The optimization problem of (3) can be solved by a constrained nonlinear programming algorithm, for example, such as the function `fmincon( )`[1] built in MATLAB.

IV. Performance Evaluation with Numerical Examples

We consider that the channel matrix $\mathbf{H}$ is calculated by using the ray-tracing method. We assume that both TX antenna elements and RX antenna elements are linearly arranged. The antenna spacing between the adjacent antenna elements is denoted as r. The distance between the center of the TX antenna array and the center of the RX antenna array is denoted as d. We assume that, throughout this paper, the transmit power is always set as such that the SNR is 20 dB when $d = 1$ m. For example, if $d = 2$ m and 10 m, then the SNR will be $20 - 6 = 14$ dB and 0 dB, respectively. Throughout this paper, the hybrid scheme will be the shared architecture, unless it is stated otherwise, because we are primarily interested in the potential (maximal) performance achieved by combining the beamforming and the spatial multiplexing.

We first consider the line-of-sight (LoS) channel, as shown in Fig. 1. We assume that both the TX antenna array line (defined as the straight line connecting all the linearly arranged antenna elements) and the RX antenna array line are perpendicular to the line connecting the centers of the TX and RX antenna arrays. The evaluated capacity of the hybrid beamforming and spatial multiplexing scheme for 2

[1] In order to use the function `fmincon( )`, the complex-valued problems should be reformulated into an equivalent real-valued problems.

$$C = \log_2 \left| \mathbf{I}_{K \times K} + \frac{E_s/N_o}{K} \left(\mathbf{V} \cdot \mathbf{W}_{\mathrm{RX}}\mathbf{H} \cdot \mathbf{W}_{\mathrm{TX}} \cdot \mathbf{U} \right) \left(\mathbf{V} \cdot \mathbf{W}_{\mathrm{RX}}\mathbf{H} \cdot \mathbf{W}_{\mathrm{TX}} \cdot \mathbf{U} \right)^{\dagger} \right| \tag{2}$$

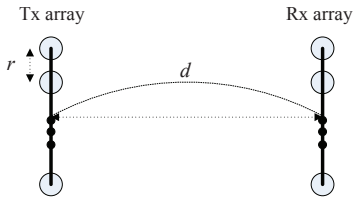

Fig. 1. TX and RX antenna arrays in a LoS channel.

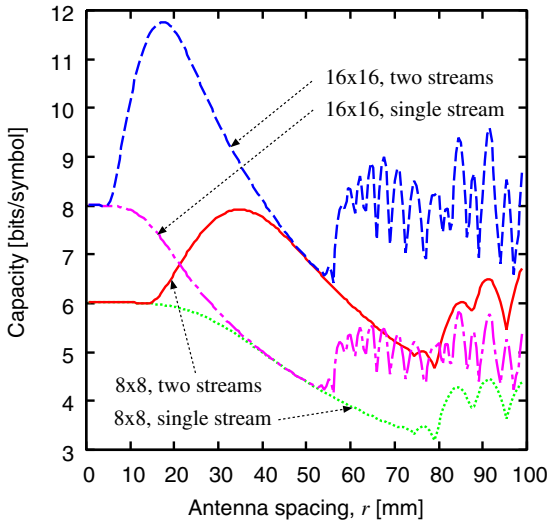

Fig. 2. Capacity comparison between single and two data streams when $d = 10$ m in the LoS channel.

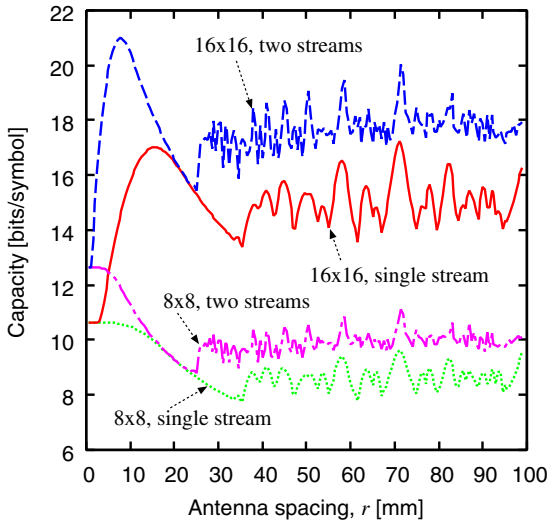

Fig. 3. Capacity comparison between single and two data streams when $d = 2$ m in the LoS channel.

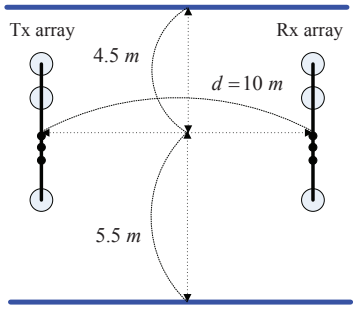

Fig. 4. TX and RX arrays in a multi-path channel with reflecting walls.

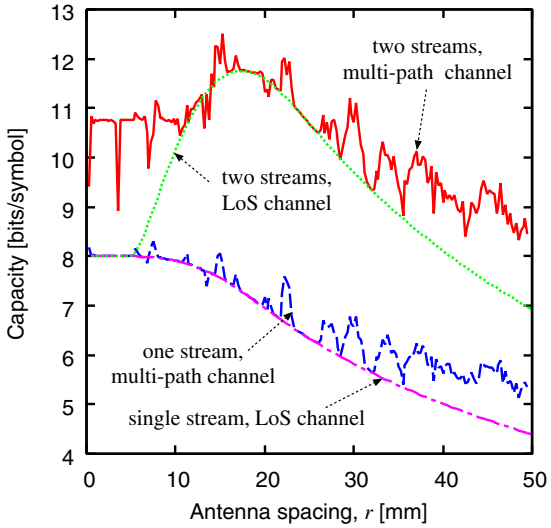

Fig. 5. Capacity comparison between the LoS and multi-path channels.

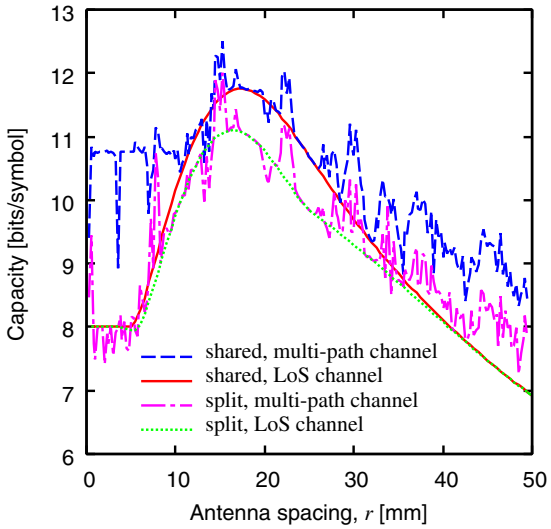

Fig. 6. Capacity comparison between the shared and split antenna architectures.

data streams is presented for $d = 10$ and 2 m in Figs. 2 and 3, respectively. The evaluated capacity of the beamforming only (BO) scheme transmitting a single data stream is also provided for comparison. While the larger antenna spacing of the BO scheme rather causes the less capacity in a region of small r, the hybrid scheme needs a somewhat large antenna spacing to obtain a desirably high capacity. The capacity gain of the hybrid scheme over the BO scheme is shown to be higher, if the number of antenna elements is larger or the distance between TX and RX is smaller.

Next we consider a multi-path channel with reflections. We assume that the antenna elements are the ideal dipole and they are vertically polarized (that is, the electric field

is perpendicular to the earth's surface). Consider a multi-path channel shown in Fig. 4, where two walls are placed on both sides of the LoS path. There are theoretically an infinite number of reflected paths between both the walls. However, we will consider only up to 2nd order reflections, neglecting the higher order reflections, as in [10]. When the vertically polarized signal is reflected from the walls in Fig. 4, it experiences a perpendicular polarization. The relative permittivity is assume to be $\epsilon_r = 1.8^2 = 3.24$, as also in [10]. The polarization type and the relative permittivity influence the reflection coefficient [10, Eq. (10)].

In Fig. 5, the evaluated capacity in the multi-path channel is compared with the LoS channel capacity for the 16×16 antenna configuration. It is noted that *even at small antenna spacing* the hybrid scheme can achieve much higher capacity than the single-stream beamforming scheme in the multi-path channel, while both schemes have similar capacities in the LoS channel.

The capacities of the shared and split antenna architectures are compared in Fig. 6. For the split antenna architecture, the optimized beamforming matrices are obtained by using the MATLAB function `fmincon( )` with 'Trust-Region-Reflective Algorithm' (the preconditioned conjugate gradient method) [19]. It is shown that degradation of the performance of the split antenna architecture compared to that of the shared antenna architecture is significant at small antenna spacing in the multi-path channel. According to such observation that the split antenna architecture (Fig. 6) with the numerically searched beamforming matrices may have smaller capacities than the BO scheme (Fig. 5), the preconditioned conjugate gradient method cannot achieve the optimal solution. The detailed discussion on how to obtain a better solution for the split antenna architecture is beyond the scope of this paper.

We will again focus only on the shared antenna architecture. Now we consider the frequency-selectivity of the capacity. The evaluated capacities for the 16×16 antenna configuration in the multi-path channel of Fig. 4 are presented over 59 to 61 GHz in Fig. 7, when $d = 10$ m and $r = 3.54$ mm[2]. The dash-dot line in Fig. 7 represents the performance of the ideal hybrid scheme, where the optimal beamforming matrices are individually obtained at each frequency (e.g., each subcarrier in an OFDM system). However, it is impractical to employ different beamforming matrices at different subcarriers, because the beamforming operations should be performed in an analog processing block. The solid and dashed lines in Fig. 7 show the performance of a more practical hybrid scheme, where a single beamforming matrix is applied to all subcarriers and it is optimized exactly at 60 GHz. In the solid line, the power allocation is allowed to depend on the subcarrier frequency. In the dashed line, on the other hand, the power allocation optimized exactly at 60 GHz is applied to all subcarriers. For the hybrid scheme, those three systems are shown to have evidently different capacities in this channel condition.

[2]This value of the antenna spacing is arbitrally chosen as such a value to produce highly frequency-selective performance.

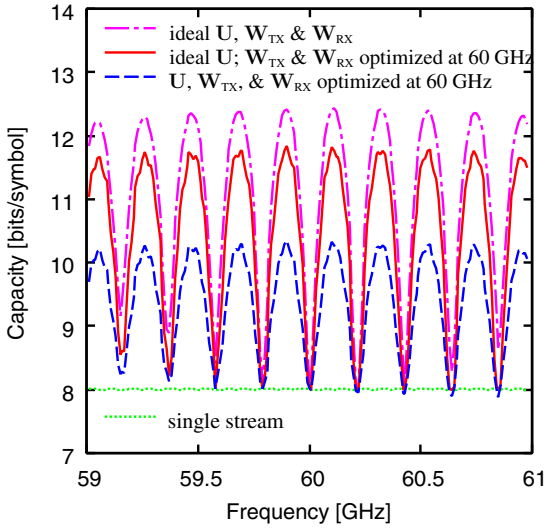

Fig. 7. Frequency-selectivity of the capacity when $r = 3.54$ mm and practical beamforming matrices are optimized *at 60 GHz*.

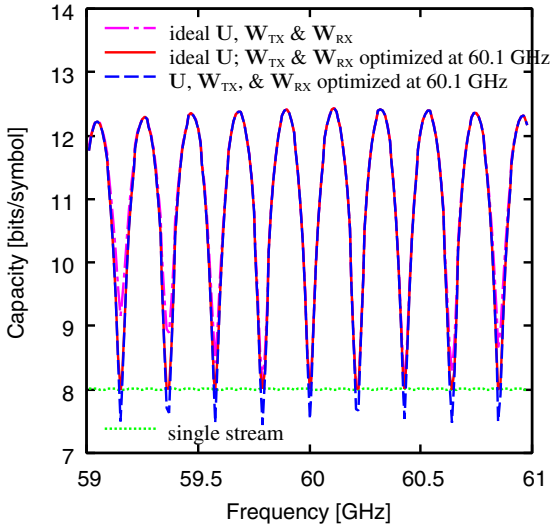

Fig. 8. Frequency-selectivity of the capacity when $r = 3.54$ mm and practical beamforming matrices are optimized *at 60.1 GHz*.

The dotted line shows the evaluated capacity of the BO scheme. For the BO scheme, the capacity and the beamforming vector are found to be almost frequency-independent. The evaluated capacities of the ideal and practical schemes are indistinguishable for the BO scheme and thus only the capacity of the ideal scheme is shown in the dotted line.

Fig. 8 is concerned with the same situation as Fig. 7, except that the beamforming matrices and the allocated powers are optimized exactly at 60.1 GHz instead of 60 GHz in non-ideal systems. It is seen that the practical system has the almost same capacity as the ideal system when the capacity is relatively high (as in the regions of local maximum points) but there are some points where the system optimized at 60.1 GHz has rather lower capacity than the system optimized at 60 GHz (as in the regions of local minimum points).

The cases such as in Figs. 7 and 8 where both the capacity

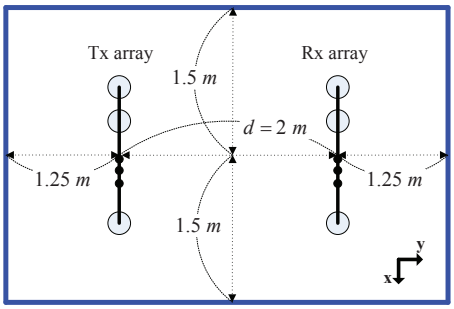

Fig. 9. TX and RX antenna arrays on the floor plan of the conference room.

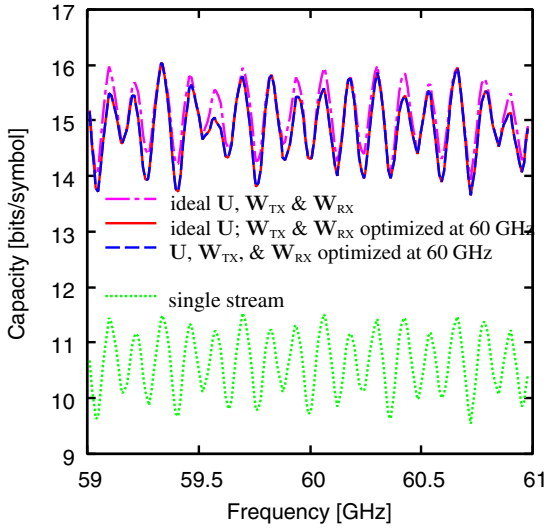

Fig. 10. Frequency-selectivity of the capacity in the channel of Fig. 9 when $r = 2.5$ mm.

and the optimal beams and powers are significantly frequency-selective are not very usual. The more common cases are where the capacity or the optimal beams and powers are approximmately frequency-nonselective, although they are not shown here due to space limitations.

Fig. 9 shows a floor plan where TX and RX antenna arrays are placed on a table in the conference room of [10, Figure 4] and where the table of [10, Figure 4] not shown in Fig. 9 is assumed to be parallel to the x-y plane. The 1st reflection from the ceiling experiences the parallel polarization and the 2nd reflection from both a wall and the ceiling experiences both perpendicular and parallel polarizations. Channel matrices based on the ray-tracing technique should be calculated considering such polarization effects as in [10, Eqs. (4) and (5)]. Reflection from the table is neglected as in [10], because the antenna is too close to the table. Fig. 10 shows the evaluated capacity for the system of the 8×8 antenna configuration in the model of Fig. 9. It is seen that the capacity is quite frequency-selective but the optimal beamforming matrices and allocated powers are not significantly sensitive to frequency.

V. Conclusion

The capacity for the hybrid transmission scheme of beamforming and spatial multiplexing was evaluated in LoS and multi-path channels. The hybrid scheme was observed to outperform the BO scheme. Its capacity gain depends on the channel parameters such as the antenna spacing, the existence of reflecting paths, etc. Especially, it was noticed that the required antenna spacing for achieving high capacity of the hybrid scheme is smaller in the multi-path channel than in the LoS channel. The frequency-selectivity of the capacity and the optimal beams and powers was seen to depend on the channel parameters. They all might be either frequency-selective or almost frequency-independent. The case was also found where the capacity is frequency-selective but the optimal beams and powers are not so sensitive to the frequency.

References

[1] R. C. Daniels and R. W. Heath, Jr., "60 GHz wireless communications: Emerging requirements and design recommendations," *IEEE Veh. Technol. Mag.,* vol. 2, no. 3, pp. 41–50, Sep. 2007.

[2] H. Singh, J. Oh, C. Y. Kweon, X. Qin, H.-R. Shao, and C. Ngo, "A 60 GHz wireless network for enabling uncompressed video communication," *IEEE Commun. Mag.,* vol. 46, no. 12, pp. 71–78, Dec. 2008.

[3] T. Baykas, C-S. Sum, Z. Lan, J. Wang, M. A. Rahman, H. Harada, and S. Kato, "IEEE 802.15.3c: The first IEEE wireless standard for data rates over 1 Gb/s," *IEEE Commun., Mag.,* vol. 49, no. 7, pp. 114–121, July 2011.

[4] Standard ECMA-387, *High Rate 60 GHz PHY, MAC and HDMI PAL,* 1st edition, Dec. 2008.

[5] C. J. Hansen, "WiGig: Multi-gigabit wireless communications in the 60 GHz band," *IEEE Wireless Commun.,*, vol. 18, no. 6, pp. 6–7, Dec. 2011.

[6] *WirelessHD Specification Version 1.1 Overview,* Available: http://www.wirelesshd.org/pdfs/WirelessHD-Specification-Overview-v1.1May2010.pdf

[7] IEEE 802.11ad, *Very High Throughput in 60 GHz*, http://www.ieee802.org/11/Reports/tgad_update.htm

[8] E. Telatar, "Capacity of multi-antenna Gaussian channels," *Europ. Trans. Telecommun.,* vol. 10, no. 6, pp. 585–595, Nov.–Dec. 1999.

[9] G. J. Foschini and M. J. Gans, "On limits of wireless communications in a fading environment when using multiple antennas," *Wireless Personal Commun.,* vol. 6, no. 3, pp. 311–335, Mar. 1998.

[10] "Channel models for 60 GHz WLAN systems," *IEEE 802.11-09/0334r8*, May 2010.

[11] S. J. Lee, K. Kim, K. Chang, M. G. Kyeong, W. Lee and H. K. Chung, "Evaluation of 60 GHz MIMO channel capacity in the conference room STA-STA scenario," in *Proc. IEEE VTC Spring*, 2011.

[12] E. Torkildson, U. Madhow, and M. Rodwell, "Indoor millimeter wave MIMO: Feasibility and performance," *IEEE Trans. Wireless Commun.,* vol. 10, no. 12, pp. 4150–4160, Dec. 2011.

[13] F. Bøhagen, P. Orten, and G. E. Øien, "Design of optimal high-rank line-of-sight MIMO channels," *IEEE Trans. Wireless Commun.,* vol. 6, no. 4, pp. 1420–1425, Apr. 2007.

[14] I. Sarris and A. R. Nix, "Design and performance assessment of high-capacity MIMO architectures in the presence of a line-of-sight component," *IEEE Trans. Veh. Technol.,* vol. 56, no. 4, pp. 2194–2202, July 2007.

[15] C. Liu, E. Skafidas, and R. J. Evans, "Capacity and data rate for millimeter wavelength systems in a short range package radio transceiver," *IEEE Trans. Wireless Commun.,* vol. 9, no. 3, pp. 903–906, Mar. 2010.

[16] A. Arvanitis, G. Anagnostou, N. Moraitis, and P. Constantinou, "Capacity study of a multiple element antenna configuration in an indoor wireless channel at 60 GHz," in *Proc. IEEE VTC2007-Spring*, 2007.

[17] N. Lashkarian, K. Nassiri-Toussi, P. Jula, and S. Kiaei, "Performance bound on ergodic capacity of MIMO beam-forming in indoor multi-path channels," *IEEE Trans. Commun.,* vol. 58, no. 11, pp. 3254–3255, Nov. 2010.

[18] M. Jiang, G. Yue, and S. Rangarajan, "MIMO transmission with rank adaptation for multi-gigabit 60GHz Wireless," in *Proc. IEEE GLOBECOM*, 2010.

[19] http://www.mathworks.co.kr/help/toolbox/optim/ug/fmincon.html.